

Thermodynamic photoinduced disorder in AlGaN nanowires

Nasir Alfaraj, Mufasila Mumthaz Muhammed, Kuang-Hui Li, Bilal Janjua, Renad A. Aljefri, Haiding Sun, Tien Khee Ng, Boon S. Ooi, Iman S. Roqan, and Xiaohang Li

Citation: [AIP Advances](#) **7**, 125113 (2017);

View online: <https://doi.org/10.1063/1.5003443>

View Table of Contents: <http://aip.scitation.org/toc/adv/7/12>

Published by the [American Institute of Physics](#)

HAVE YOU HEARD?

Employers hiring scientists and
engineers trust

PHYSICS TODAY | JOBS

www.physicstoday.org/jobs



Thermodynamic photoinduced disorder in AlGaN nanowires

Nasir Alfaraj,¹ Mufasila Mumthaz Muhammed,² Kuang-Hui Li,¹ Bilal Janjua,³ Renad A. Aljefri,¹ Haiding Sun,¹ Tien Khee Ng,³ Boon S. Ooi,³ Iman S. Roqan,^{2,a} and Xiaohang Li^{1,b}

¹Advanced Semiconductor Laboratory, King Abdullah University of Science and Technology (KAUST), Thuwal 23955-6900, Kingdom of Saudi Arabia

²Semiconductor and Material Spectroscopy Laboratory, King Abdullah University of Science and Technology (KAUST), Thuwal 23955-6900, Kingdom of Saudi Arabia

³Photonics Laboratory, King Abdullah University of Science and Technology (KAUST), Thuwal 23955-6900, Kingdom of Saudi Arabia

(Received 6 September 2017; accepted 4 December 2017; published online 13 December 2017)

In this study, we examine thermodynamic photoinduced disorder in AlGaN nanowires through their steady-state and transient photoluminescence properties. We correlate the energy exchange during the photoexcitation and photoemission processes of the light–solid reaction and the generation of photoinduced entropy of the nanowires using temperature-dependent (6 K to 290 K) photoluminescence. We observed an oscillatory trend in the generated entropy of the system below 200 K, with an oscillation frequency that was significantly lower than what we have previously observed in InGaN/GaN nanowires. In contrast to the sharp increase in generated entropy at temperatures close to room temperature in InGaN/GaN nanowires, an insignificant increase was observed in AlGaN nanowires, indicating lower degrees of disorder-induced uncertainty in the wider bandgap semiconductor. We conjecture that the enhanced atomic ordering in AlGaN caused lower degrees of disorder-induced uncertainty related to the energy of states involved in thermionic transitions; in keeping with this conjecture, we observed lower oscillation frequency below 200 K and a stable behavior in the generated entropy at temperatures close to room temperature. © 2017 Author(s). All article content, except where otherwise noted, is licensed under a Creative Commons Attribution (CC BY) license (<http://creativecommons.org/licenses/by/4.0/>). <https://doi.org/10.1063/1.5003443>

I. INTRODUCTION

Combining several forms of inorganic compounds based on silicon and group-III-nitride semiconductor materials into one electronic system has shown promise for revolutionizing the electronics industry.^{1–5} Realizing AlGaN nanowire-based, high-performance, and droop-free ultraviolet (UV) semiconductor optoelectronic devices with complex heterostructures is now possible thanks to the nanowire sidewall strain relaxation, which allows for the integration of lattice-mismatched group-III-nitride materials without creating dislocations.^{6–8} Using a variety of growth techniques,^{9,10} AlN and its alloys $\text{Al}_x\text{Ga}_{1-x}\text{N}$ ($0 < x \leq 1$) are expected to facilitate the fabrication of more sensitive UV photodetector devices,^{11,12} ultralow-threshold UV lasers,¹³ and reduce polarization fields.^{14,15}

GaN-based nanowire devices have high quantum efficiencies,^{16,17} sharp peaks of density of states at the lowest quantized sub-band energy levels,¹⁸ improved exciton binding energy,¹⁹ and increased wavefunction overlap of the electron-hole pairs.²⁰ Moreover, designing heterojunction-based optoelectronic devices through the integration of three-dimensional (3D) group-III-nitride

^aElectronic mail: iman.roqan@kaust.edu.sa

^bElectronic mail: xiaohang.li@kaust.edu.sa

materials with two-dimensional (2D) transition metal dichalcogenide layers is now possible after determining their band offset parameters.^{21–24} Connie *et al.* investigated the optical and electrical properties of deep-UV (DUV) magnesium-doped AlN nanowires with a low magnesium acceptor thermal activation energy of 23 meV within the temperature range of 300 K–450 K.²⁵ They argued that the *p*-type conduction is dominated by hopping conduction. Still, in the absence of common impurity incorporation and vacancy centers, such as the growth-induced formation of carbon impurities^{26,27} and nitrogen-vacancy related defects,²⁵ non-radiative surface recombination affects the performance of nanowire devices grown using molecular beam epitaxy (MBE), as the quantum efficiency of nanowire optoelectronic devices can be limited by the increased density of surface trap states (Shockley–Read–Hall recombination)²⁸ and the filling of inner-shell vacancies (Auger recombination).²⁹

GaN-based nanowires have recently emerged as the center of attention as potential building blocks for future nanostructured long-term stable opto-electrothermal devices.^{30–32} Even though GaN nanowire-based devices, including tunnel-injected DUV light-emitting diodes (LEDs)³³ and LEDs for monolithic metal-optoelectronics³⁴ and high-power light emitters,³⁵ have recently been realized, understanding and optimizing the electrothermal characteristics^{36,37} of GaN-based nanowires is critical for identifying and achieving their full potential in opto-electrothermal device applications.^{38,39} As a consequence of the thermal activation of non-radiative recombination channels, we observed an increasing trend in the amount of generated photoinduced entropy of the InGaN nanowire system as its temperature approached room temperature, which is a valid assessment of the thermodynamic disorder in photoluminescent semiconducting materials.⁴⁰ Furthermore, the non-radiative photocarrier recombination lifetimes in nanostructured materials are naturally shorter than those of bulk structures owing to their higher surface-to-volume ratios.

II. EXPERIMENTAL RESULTS AND DISCUSSION

A. Sample description and experimental setup

We utilized temperature-dependent photoluminescence (PL) to investigate the photoinduced entropy of AlGaN nanowires. We recalled our definition of photoinduced entropy as a thermodynamic measure of the unavailability of a system's energy for conversion into useful work because of luminescence refrigeration.^{40–42} We also examined the dynamics of photocarriers using time-resolved photoluminescence (TRPL) down to the picosecond regime. Fig. 1(A) depicts the schematic layer structure of our AlGaN nanowires, with the *c*-axis along the direction of growth normal to the silicon substrate surface. The nanowires were grown using plasma-assisted MBE.^{35,40} The nanowires consisted of 10 nm unintentionally-doped GaN nanobuffers and approximately 290 nm unintentionally doped AlGaN layers grown sequentially. Before the growth of AlGaN, thin GaN nanowire array template was grown to promote the formation of AlGaN nanowires.⁴³

We measured the PL and TRPL using a frequency-tripled Ti:sapphire laser with a pulse width (τ_{on}) of 130 fs and a syncroskan streak-camera system. A third harmonic generator, with an output wavelength (λ_{ex}) of 266 nm and a pulse repetition rate (f_{rep}) of 76 MHz, was employed to excite the sample. The TRPL measurements were used to examine the carrier lifetimes in the AlGaN nanowires over a temperature (T) range from 6 K to 290 K. The overall temporal resolution of our setup was 10 ps. Fig. 1(B) depicts a tilted plan-view scanning electron microscope (SEM) image, with a nanowire mean top cross-sectional size ($2r_{\text{NW}}$) of 55 nm, while Fig. 1(C) shows a tilted cross-sectional-view SEM image of the nanowires. The larger diameter nanowires could be due to bundling effects.^{44,45}

B. Steady-state and transient photoluminescence measurements

In Fig. 2 and Fig. 3, we present typical luminescence PL spectra and TRPL decay curves, respectively, for an ensemble of AlGaN nanowires at various temperatures. Charge carrier dynamics (e.g. the characteristic charge carrier mobility and lifetime) reflect the nature and quality of semiconductor device materials,⁴⁶ and is influenced by device architecture, the nature and dimensions of the materials and interfaces involved, and operational mode.⁴⁷ Examples include semiconducting zero-dimensional (0D) nanocrystals (NCs) and quantum dots (QDs),^{48,49} 1D nanowire

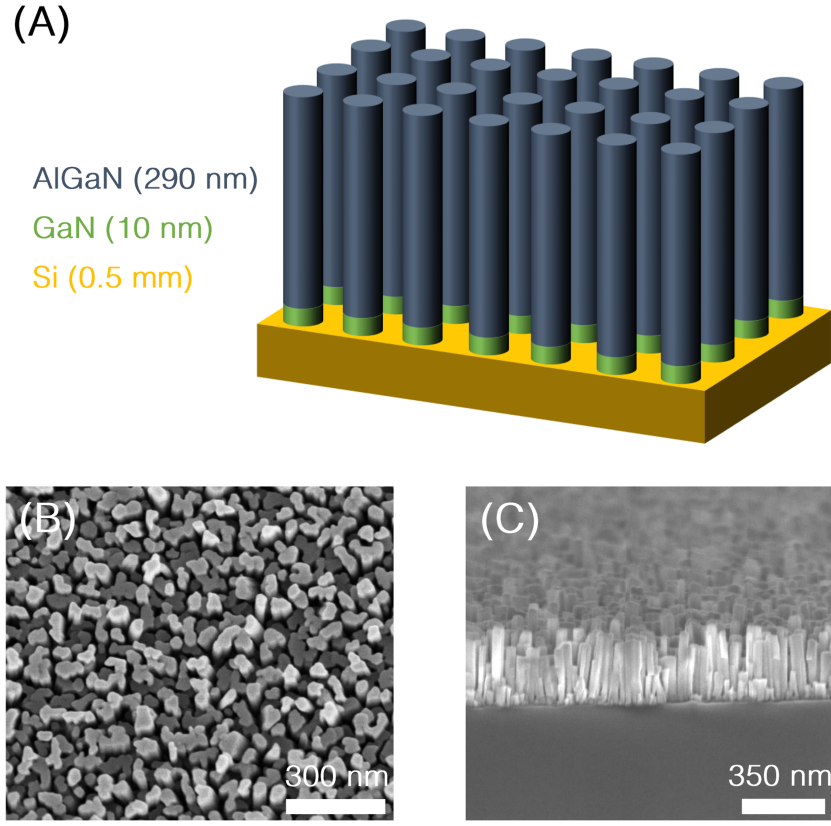


FIG. 1. (A) Schematic and layer structure of the AlGaN nanowires. (B) Tilted plan-view and (C) tilted cross-sectional-view SEM images of the nanowires.

solar cells,⁵⁰ two-dimensional (2D) GaN,⁵¹ and three-dimensional (3D) InGaN/GaN core–shell nanorods⁵² and nanoscale silicon-based transistors,^{53,54} which can demonstrate opto-electrical, photovoltaic, and signal switching properties superior to those of their bulk and large-area counterparts.

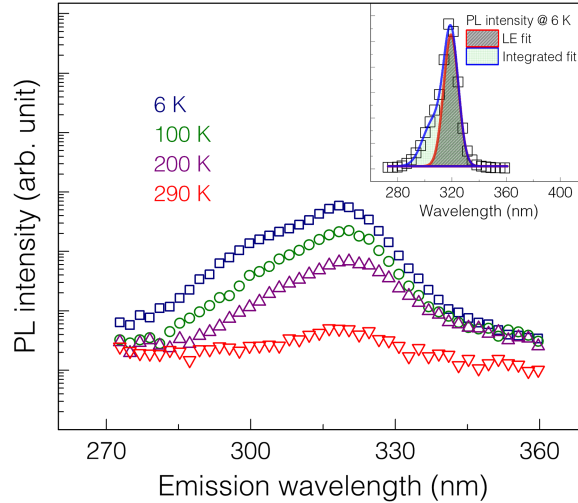


FIG. 2. Typical semilogarithmic scale PL spectra for the AlGaN nanowires at various temperatures from 6 K and 290 K. In the inset, we fitted a Gaussian model to the linear scale PL data at 6 K to distinguish the dominant LE peak from the integrated PL emission.

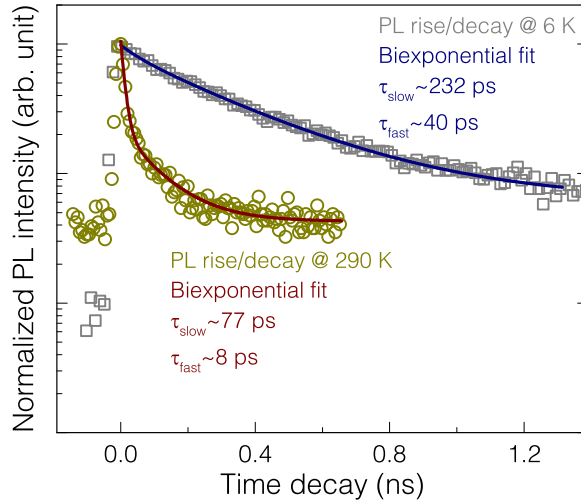


FIG. 3. Typical semilogarithmic scale AlGaN-related TRPL decay curves for the AlGaN nanowires at 6 K and 290 K with biexponential fits.

In particular, surface states on group III-V nanowire-based photodetectors, in addition to the presence of impurities and defect sites, can introduce a serious degradation in the free charge carrier lifetime.⁵⁵

We analyzed the TRPL decay curves using a biexponential decay model. This model provided the most proper fit because of its multi-center recombination characteristics as it accounted for carrier capture and relaxation processes in a multilevel system.^{56–58} In other words, the biexponential model best fit the ultrafast carrier thermalization dynamics (the initial fast decay) and the slower carrier cooling effects⁵⁹ (slow decay) that were characteristic of our measured AlGaN nanowires, thus enabling individual analysis of fast and slow components.⁶⁰

Using Vegard's law, the aluminum composition in the AlGaN nanowires was calculated and found to be approximately 18%. We fitted our TRPL decay curves using a biexponential decay model because it better depicted the multiple recombination characteristics exemplified by the curves.^{61,62} Typically, Auger recombination is negligibly small in wide-bandgap semiconductors.⁶³

C. Carrier localization and photoinduced entropy

Fig. 4(A) shows the peak energy of emission ($E_{\text{PL, peak}}$) curves of the integrated and low-energy (LE) peak-related PL emissions from the Al_{0.18}Ga_{0.82}N nanowires, while Fig. 4(B) and Fig. 4(C) display the integrated PL intensities ($E_{\text{PL, intg}}$) and spectral width (λ_{FWHM}), respectively, as a function of temperature. Between 6 K and 150 K, we observed a redshift in $E_{\text{PL, intg}}$, which we attributed to thermal relaxation of electric charges induced by spontaneous and piezoelectric polarization fields.⁶⁴ Beyond 150 K, band-filling⁶⁵ and/or grain boundary excitonic localization effects may have started to dominate, and hence we observed a blueshift in $E_{\text{PL, intg}}$.⁶⁶ Ajia *et al.* found that as the aluminum content decreased in metalorganic chemical vapor deposition (MOCVD)-grown AlGaN/AlGaN multiquantum-wells (MQWs), the average height of the grains decreased while the average diameter of the grains increased, which caused localization within the grain boundaries and hence the blueshift above 150 K. Such behavior was attributed to the disparity in the respective adsorption rates of gallium and aluminum adatoms. Grain boundaries were found to exist in MBE-grown GaN nanowires.⁶⁷ Motayed *et al.* reported that grain boundaries can exist in MBE-grown GaN nanowires, although their effects on carrier transport properties diminished as their diameter became smaller.⁶⁸

In Fig. 5(A), we show the slow-component of the total carrier recombination lifetimes ($\tau_{\text{PL, slow}}$) extracted from fitting the biexponential decay model to the TRPL data, which gradually drop as the temperature increases. At low temperatures (i.e. between 6 K to 80 K), the measured lifetime fluctuated between 222 ps and 238 ps. The decrease in lifetime with increasing temperature indicates

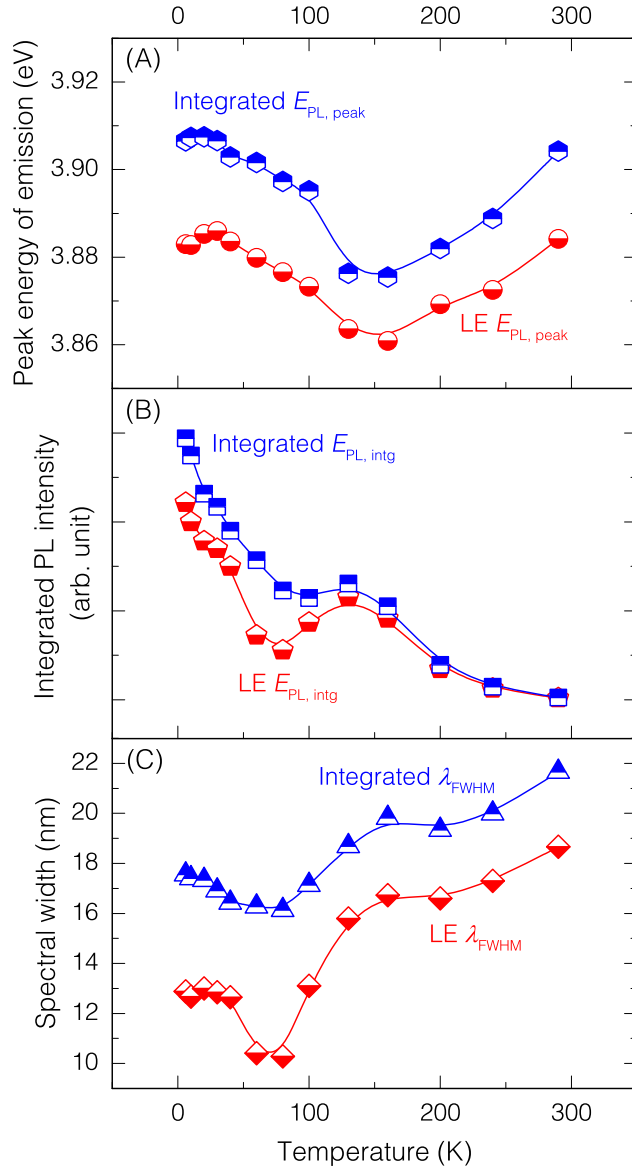


FIG. 4. (A) Cumulative and LE peak-related $E_{PL, peak}$, (B) $E_{PL, intg}$, and (C) their respective PL emissions λ_{FWHM} plots as a function of temperature.

that the non-radiative contribution decreases, which we attribute to surface defect states.⁶⁹ Because quantum confinement effects are absent in our nanowires, less efficient radiative recombination of photoexcited carriers is achieved, although the possible presence of grain-boundary-induced carrier localization effects enhances the radiative recombination efficiency. As we previously noted,⁴⁰ the entropy of a system sets an upper limit on the number of emitted photons from an active region and is always positive—emitted photons transport entropy produced by the absorption of heat from the active region.^{70–72} We recall our definition of the change in entropy S due to photoexcitation and photoemission⁴⁰

$$S(E_{j+1}) \approx S(E_j) + 2 \frac{(E_{j+1}^{PL, intg} - E_j^{PL, intg})}{T_{j+1} + T_j}, \quad (1)$$

where E_j is the total energy of the system at temperature T_j . Put differently, we let $E_1 < \dots < E_{13}$ denote the sorted total energies, and T_j be the system temperatures corresponding to each E_j .

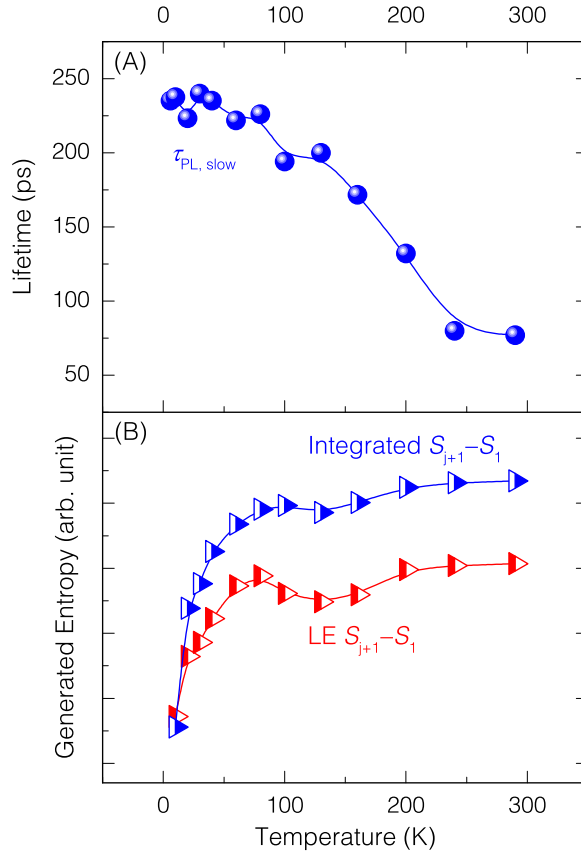


FIG. 5. (A) The extracted $\tau_{PL, slow}$ values of the AlGaN nanowires as a function of temperature and (B) the integrated and LE-peak-related evolution of the amount of entropy generation with temperature.

As Fig. 5(B) shows, the evolution in the entropy generation curve manifested an oscillatory trend between 6 K and 200 K, with an oscillation frequency that was significantly lower than what we previously observed in $In_{0.32}Ga_{0.68}N$.⁴⁰ The oscillatory trend stabilized after 200 K. In contrast to what we previously observed in $In_{0.32}Ga_{0.68}N$, there was no significant increase in the amount of generated entropy as the temperature approached room temperature. In the presence of non-radiative recombination centers in our nanowires caused by surface states and other defects, we expected additional entropy to be generated because of the irreversible nature of non-radiative processes.^{70,73} However, in our present case, entropy generation was nearly constant above 200 K. We hypothesize that surface defect states dominantly contributed to entropy generation above this temperature, and conjecture that the $Al_{0.18}Ga_{0.82}N$ alloy composition fluctuations,⁷⁴ which are intrinsic in localized states that are present in only very small sections (<2 nm),⁷⁵ contributed to the lower degrees of disorder-induced uncertainty related to the energy of states involved in thermionic transitions at higher temperatures because of the effects of atomic ordering.⁷⁶⁻⁷⁸ To support this hypothesis, we fitted the following stretched-exponential decay model to our TRPL decay curves

$$I(t, T_j) = I(0, T_j) e^{(-t/\tau_{PL, str})^{\beta(T_j)}}, \quad (2)$$

where $I(t, T_j)$ is the TRPL intensity as a function of time and temperature, and $\beta(T_j)$ is the stretching parameter (between 0 and 1) at temperature T_j . The latter is linked to the distribution of the carrier localization centers.⁷⁹ This model, which has widely been used to describe the dynamics of heavily disordered systems,^{80,81} provides a direct measurement of the effects of high excitation carrier density and disorder within the material,⁸² such as compositional variation in nanowires.³⁴ As can be seen in Fig. 6, β varied between 0.63 and 0.88 over a wide range of temperatures, while it fluctuated

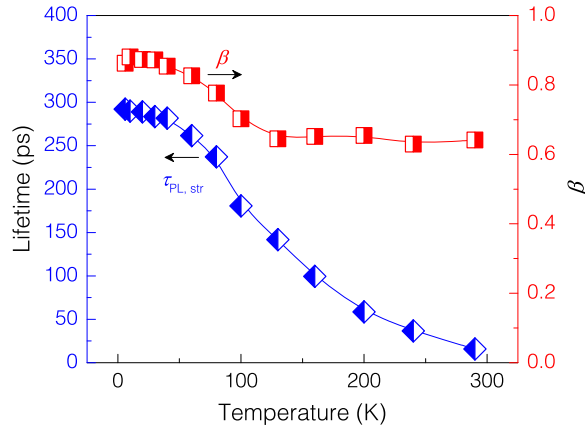


FIG. 6. The extracted $\tau_{PL, str}$ and β values of the AlGaN nanowires as a function of temperature.

between 0.63 and 0.65 at temperatures above 100 K, indicating a behavior that was nearly independent of T , therefore confirming the low compositional disorder within the measured $\text{Al}_{0.18}\text{Ga}_{0.82}\text{N}$ nanowires.

III. CONCLUDING REMARKS

In summary, we investigated the photoinduced entropy of $\text{Al}_{0.18}\text{Ga}_{0.82}\text{N}$ nanowires and analyzed the related photocarrier dynamics. We observed an oscillatory trend in the generated entropy of the system below 200 K, with an oscillation frequency that was significantly lower than what was previously observed in $\text{In}_{0.32}\text{Ga}_{0.68}\text{N}$ nanowires. Moreover, we did not observe any sharp increase in generated entropy at temperatures close to room temperature in $\text{Al}_{0.18}\text{Ga}_{0.82}\text{N}$ in contrast to what was observed in the measured $\text{In}_{0.32}\text{Ga}_{0.68}\text{N}$ nanowires. We hypothesize that the increased atomic ordering in $\text{Al}_{0.18}\text{Ga}_{0.82}\text{N}$, compared to that in $\text{In}_{0.32}\text{Ga}_{0.68}\text{N}$, caused the lower oscillation frequency below 200 K and the stable behavior in the generated entropy at temperatures close to room temperature.

This publication is based upon work supported by the King Abdullah University of Science and Technology (KAUST) baseline funding, BAS/1/1664-01-01 and BAS/1/1647-01-05. B.J., T.K.N., and B.S.O. acknowledge the financial support from King Abdulaziz City for Science and Technology (KACST), Grant No. KACST TIC R2-FP-008, and KAUST baseline funding, BAS/1/1614-01-01.

- ¹ S.-i. Inoue, N. Tamari, and M. Taniguchi, *Appl. Phys. Lett.* **110**, 141106 (2017).
- ² A. W. Bruch, K. Xiong, H. Jung, X. Guo, C. Zhang, J. Han, and H. X. Tang, *Appl. Phys. Lett.* **110**, 021111 (2017).
- ³ T. Yamada, J. Ito, R. Asahara, K. Watanabe, M. Nozaki, T. Hosoi, T. Shimura, and H. Watanabe, *Appl. Phys. Lett.* **110**, 261603 (2017).
- ⁴ B. Janjua, T. K. Ng, C. Zhao, H. M. Oubei, C. Shen, A. Prabaswara, M. S. Alias, A. A. Alhamoud, A. A. Alatawi, A. M. Albadri, A. Y. Alyamani, M. M. El-Desouki, and B. S. Ooi, *Opt. Express* **24**, 19228 (2016).
- ⁵ M. Gadalla, M. Abdel-Rahman, and A. Shamim, *Sci. Rep.* **4**, 4270 (2014).
- ⁶ M. Conroy, V. Z. Zubialevich, H. Li, N. Petkov, S. O'Donoghue, J. D. Holmes, and P. J. Parbrook, *ACS Nano* **10**, 1988 (2016).
- ⁷ B. Janjua, H. Sun, C. Zhao, D. H. Anjum, D. Priante, A. A. Alhamoud, F. Wu, X. Li, A. M. Albadri, A. Y. Alyamani, M. M. El-Desouki, T. K. Ng, and B. S. Ooi, *Opt. Express* **25**, 1381 (2017).
- ⁸ F. Glas, *Wide Band Gap Semiconductor Nanowires I* (John Wiley and Sons, Inc., 2014), pp. 25–57.
- ⁹ S. Zhao, S. Y. Woo, S. M. Sadaf, Y. Wu, A. Pofelski, D. A. Laleyan, R. T. Rashid, Y. Wang, G. A. Botton, and Z. Mi, *APL Mater.* **4**, 086115 (2016).
- ¹⁰ M. Conroy, V. Z. Zubialevich, H. Li, N. Petkov, J. D. Holmes, and P. J. Parbrook, *J. Mater. Chem. C* **3**, 431 (2015).
- ¹¹ X. Zhang, Q. Liu, B. Liu, W. Yang, J. Li, P. Niu, and X. Jiang, *J. Mater. Chem. C* (2017).
- ¹² N. Aggarwal, S. Krishna, A. Sharma, L. Goswami, D. Kumar, S. Husale, and G. Gupta, *Adv. Electron. Mater.* **3** (2017).
- ¹³ K. Li, X. Liu, Q. Wang, S. Zhao, and Z. Mi, *Nat. Nanotechnol.* **10**, 140 (2015).
- ¹⁴ A. Gundimeda, S. Krishna, N. Aggarwal, A. Sharma, N. D. Sharma, K. Maurya, S. Husale, and G. Gupta, *Appl. Phys. Lett.* **110**, 103507 (2017).
- ¹⁵ B. H. Le, S. Zhao, X. Liu, S. Y. Woo, G. A. Botton, and Z. Mi, *Adv. Mater.* **28**, 8446 (2016).

- ¹⁶ D. Banerjee, S. Sankaranarayanan, D. Khachariya, M. B. Nadar, S. Ganguly, and D. Saha, *Appl. Phys. Lett.* **109**, 031111 (2016).
- ¹⁷ F. Qian, S. Gradecak, Y. Li, C.-Y. Wen, and C. M. Lieber, *Nano Lett.* **5**, 2287 (2005).
- ¹⁸ J. Mao, Z. Liu, and Z. Ren, *NPJ Quantum Mater.* **1**, 16028 (2016).
- ¹⁹ A. Das, J. Heo, M. Jankowski, W. Guo, L. Zhang, H. Deng, and P. Bhattacharya, *Phys. Rev. Lett.* **107**, 066405 (2011).
- ²⁰ F. Wu, H. Sun, I. Ajia, I. Roqan, D. Zhang, J. Dai, C. Chen, Z. C. Feng, and X. Li, *J. Phys. D: Appl. Phys.* **50**, 245101 (2017).
- ²¹ M. Tangi, P. Mishra, M.-Y. Li, M. K. Shakfa, D. H. Anjum, M. N. Hedhili, T. K. Ng, L.-J. Li, and B. S. Ooi, *Appl. Phys. Lett.* **111**, 092104 (2017).
- ²² M. Tangi, P. Mishra, C.-C. Tseng, T. K. Ng, M. N. Hedhili, D. H. Anjum, M. S. Alias, N. Wei, L.-J. Li, and B. S. Ooi, *ACS Appl. Mater. Interfaces* **9**, 9110 (2017).
- ²³ M. Tangi, P. Mishra, T. K. Ng, M. N. Hedhili, B. Janjua, M. S. Alias, D. H. Anjum, C.-C. Tseng, Y. Shi, H. J. Joyce, L.-J. Li, and B. S. Ooi, *Appl. Phys. Lett.* **109**, 032104 (2016).
- ²⁴ P. Mishra, M. Tangi, T. K. Ng, M. N. Hedhili, D. H. Anjum, M. S. Alias, C.-C. Tseng, L.-J. Li, and B. S. Ooi, *Appl. Phys. Lett.* **110**, 012101 (2017).
- ²⁵ A. T. Connie, S. Zhao, S. M. Sadaf, I. Shih, Z. Mi, X. Du, J. Lin, and H. Jiang, *Appl. Phys. Lett.* **106**, 213105 (2015).
- ²⁶ H. Sun, F. Wu, Y. J. Park, T. M. A. Altahtamouni, K.-H. Li, N. Alfaraj, T. Detchprohm, R. D. Dupuis, and X. Li, *Appl. Phys. Lett.* **110**, 192106 (2017).
- ²⁷ H. Sun, F. Wu, T. M. A. Altahtamouni, N. Alfaraj, K. Li, T. Detchprohm, R. Dupuis, and X. Li, *J. Phys. D: Appl. Phys.* **50**, 395101 (2017).
- ²⁸ F. Olivier, A. Daami, C. Licitra, and F. Templier, *Appl. Phys. Lett.* **111**, 022104 (2017).
- ²⁹ W. Guo, M. Zhang, P. Bhattacharya, and J. Heo, *Nano Lett.* **11**, 1434 (2011).
- ³⁰ C. Yu, C. Buttay, and É. Labouré, *IEEE Trans. Power Electron.* **32**, 906 (2017).
- ³¹ J. Cho, D. Francis, D. H. Altman, M. Asheghi, and K. E. Goodson, *J. Appl. Phys.* **121**, 055105 (2017).
- ³² K. Tsuchiyama, K. Yamane, S. Utsunomiya, H. Sekiguchi, H. Okada, and A. Wakahara, *Appl. Phys. Express* **9**, 104101 (2016).
- ³³ Y. Zhang, S. Krishnamoorthy, F. Akyol, S. Bajaj, A. A. Allerman, M. W. Moseley, A. M. Armstrong, and S. Rajan, *Appl. Phys. Lett.* **110**, 201102 (2017).
- ³⁴ C. Zhao, T. K. Ng, R. T. ElAfandy, A. Prabaswara, G. B. Consiglio, I. A. Ajia, I. S. Roqan, B. Janjua, C. Shen, J. Eid, A. Y. Alyamani, M. M. El-Desouki, and B. S. Ooi, *Nano Lett.* **16**, 4616 (2016).
- ³⁵ C. Zhao, T. K. Ng, N. Wei, A. Prabaswara, M. S. Alias, B. Janjua, C. Shen, and B. S. Ooi, *Nano Lett.* **16**, 1056 (2016).
- ³⁶ V. O. Turin and A. A. Balandin, *J. Appl. Phys.* **100**, 054501 (2006).
- ³⁷ M. T. Ghoneim, H. M. Fahad, A. M. Hussain, J. P. Rojas, G. A. Torres Sevilla, N. Alfaraj, E. B. Lizardo, and M. M. Hussain, *AIP Adv.* **5**, 127115 (2015).
- ³⁸ Y. Yong, H. Jiang, X. Li, S. Lv, and J. Cao, *Phys. Chem. Chem. Phys.* **18**, 21431 (2016).
- ³⁹ M. G. Kibria, R. Qiao, W. Yang, I. Boukahil, X. Kong, F. A. Chowdhury, M. L. Trudeau, W. Ji, H. Guo, F. Himpel, L. Vayssières, and Z. Mi, *Adv. Mater.* **28**, 8388 (2016).
- ⁴⁰ N. Alfaraj, S. Mitra, F. Wu, I. A. Ajia, B. Janjua, A. Prabaswara, R. A. Aljefri, H. Sun, T. Khee Ng, B. S. Ooi, I. S. Roqan, and X. Li, *Appl. Phys. Lett.* **110**, 161110 (2017).
- ⁴¹ J.-B. Wang, S. R. Johnson, D. Ding, S.-Q. Yu, and Y.-H. Zhang, *J. Appl. Phys.* **100**, 043502 (2006).
- ⁴² P. Berdahl, *J. Appl. Phys.* **58**, 1369 (1985).
- ⁴³ S. Zhao, A. Connie, M. Dastjerdi, X. Kong, Q. Wang, M. Djavid, S. Sadaf, X. Liu, I. Shih, H. Guo, and Z. Mi, *Sci. Rep.* **5**, 8332 (2015).
- ⁴⁴ V. M. Kaganer, S. Fernández-Garrido, P. Dogan, K. K. Sabelfeld, and O. Brandt, *Nano Lett.* **16**, 3717 (2016).
- ⁴⁵ Z. de Souza Schieber, G. Calabrese, X. Kong, A. Trampert, B. Jenichen, J. H. Dias da Silva, L. Geelhaar, O. Brandt, and S. Fernández-Garrido, *Nano Lett.* **17**, 63 (2016).
- ⁴⁶ N. Alfaraj, A. M. Hussain, G. A. Torres Sevilla, M. T. Ghoneim, J. P. Rojas, A. B. Aljedaani, and M. M. Hussain, *Appl. Phys. Lett.* **107**, 174101 (2015).
- ⁴⁷ H. J. Joyce, S. A. Baig, P. Parkinson, C. L. Davies, J. L. Boland, H. H. Tan, C. Jagadish, L. M. Herz, and M. B. Johnston, *J. Phys. D: Appl. Phys.* **50**, 224001 (2017).
- ⁴⁸ L. Zhang, C.-H. Teng, P.-C. Ku, and H. Deng, *Phys. Rev. B* **93**, 085301 (2016).
- ⁴⁹ A. P. Alivisatos, *Science* **271**, 933 (1996).
- ⁵⁰ T. Lin, S. Ramadurgam, and C. Yang, *Nano Lett.* **17**, 2118 (2017).
- ⁵¹ Z. Y. Al Balushi, K. Wang, R. K. Ghosh, R. A. Vilá, S. M. Eichfeld, J. D. Caldwell, X. Qin, Y.-C. Lin, P. A. DeSario, G. Stone, S. Subramanian, D. F. Paul, R. M. Wallace, S. Datta, J. M. Redwing, and J. A. Robinson, *Nat. Mater.* **15**, 1166 (2016).
- ⁵² M. Müller, P. Veit, F. F. Krause, T. Schimpke, S. Metzner, F. Bertram, T. Mehrtens, K. Müller-Caspary, A. Avramescu, M. Strassburg, A. Rosenauer, and J. Christen, *Nano Lett.* **16**, 5340 (2016).
- ⁵³ J. P. Rojas, G. A. Torres Sevilla, N. Alfaraj, M. T. Ghoneim, A. T. Kutbee, A. Sridharan, and M. M. Hussain, *ACS Nano* **9**, 5255 (2015).
- ⁵⁴ M. T. Ghoneim, N. Alfaraj, G. A. Torres-Sevilla, H. M. Fahad, and M. M. Hussain, *IEEE Trans. Electron Dev.* **63**, 2657 (2016).
- ⁵⁵ X. Yan, B. Li, Y. Wu, X. Zhang, and X. Ren, *Appl. Phys. Lett.* **109**, 053109 (2016).
- ⁵⁶ O. Brandt, J. Ringling, K. H. Ploog, H.-J. Wünsche, and F. Henneberger, *Phys. Rev. B* **58**, R15977 (1998).
- ⁵⁷ O. Brandt, B. Yang, H.-J. Wünsche, U. Jahn, J. Ringling, G. Paris, H. Grahn, and K. Ploog, *Phys. Rev. B* **58**, R13407 (1998).
- ⁵⁸ A. Gorgis, T. Flissikowski, O. Brandt, C. Chèze, L. Geelhaar, H. Riechert, and H. T. Grahn, *Phys. Rev. B* **86**, 041302 (2012).
- ⁵⁹ J. Hamazaki, H. Kunugita, K. Ema, A. Kikuchi, and K. Kishino, *Phys. Rev. B* **71**, 165334 (2005).

- ⁶⁰L. Liu, L. Wang, N. Liu, W. Yang, D. Li, W. Chen, Z. C. Feng, Y.-C. Lee, I. Ferguson, and X. Hu, *J. Appl. Phys.* **112**, 083101 (2012).
- ⁶¹M. Muhammed, M. Roldan, Y. Yamashita, S.-L. Sahonta, I. A. Ajia, K. Iizuka, A. Kuramata, C. Humphreys, and I. S. Roqan, *Sci. Rep.* **6**, 29747 (2016).
- ⁶²S. Jain, M. Willander, J. Narayan, and R. Van Overstraeten, *J. Appl. Phys.* **87**, 965 (2000).
- ⁶³H. Yoshida, M. Kuwabara, Y. Yamashita, K. Uchiyama, and H. Kan, *Appl. Phys. Lett.* **96**, 211122 (2010).
- ⁶⁴O. Ambacher, J. Smart, J. R. Shealy, N. G. Weimann, K. Chu, M. Murphy, W. J. Schaff, L. F. Eastman, R. Dimitrov, L. Wittmer, M. Stutzmann, W. Rieger, and J. Hilsenbeck, *J. Appl. Phys.* **85**, 3222 (1999).
- ⁶⁵S.-H. Park and S.-L. Chuang, *Appl. Phys. Lett.* **76**, 1981 (2000).
- ⁶⁶I. A. Ajia, P. R. Edwards, Z. Liu, J. C. Yan, R. W. Martin, and I. S. Roqan, *Appl. Phys. Lett.* **105**, 122111 (2014).
- ⁶⁷R. A. Bernal, R. Agrawal, B. Peng, K. A. Bertness, N. A. Sanford, A. V. Davydov, and H. D. Espinosa, *Nano Lett.* **11**, 548 (2010).
- ⁶⁸A. Motayed, M. Vaudin, A. V. Davydov, J. Melngailis, M. He, and S. Mohammad, *Appl. Phys. Lett.* **90**, 043104 (2007).
- ⁶⁹H. P. T. Nguyen, S. Zhang, A. T. Connie, M. G. Kibria, Q. Wang, I. Shih, and Z. Mi, *Nano Lett.* **13**, 5437 (2013).
- ⁷⁰A. David, C. A. Hurni, N. G. Young, and M. D. Craven, *Appl. Phys. Lett.* **109**, 083501 (2016).
- ⁷¹M. Weinstein, *J. Opt. Soc. Am.* **50**, 597 (1960).
- ⁷²P. Landsberg and G. Tonge, *J. Appl. Phys.* **51**, R1 (1980).
- ⁷³J. Xue, Z. Li, and R. J. Ram, *Phys. Rev. Applied* **8**, 014017 (2017).
- ⁷⁴C.-K. Li, M. Piccardo, L.-S. Lu, S. Mayboroda, L. Martinelli, J. Peretti, J. S. Speck, C. Weisbuch, M. Filoche, and Y.-R. Wu, *Phys. Rev. B* **95**, 144206 (2017).
- ⁷⁵M. Belloeil, B. Gayral, and B. Daudin, *Nano Lett.* **16**, 960 (2016).
- ⁷⁶S. Zhao, S. Woo, M. Bugnet, X. Liu, J. Kang, G. Botton, and Z. Mi, *Nano Lett.* **15**, 7801 (2015).
- ⁷⁷S. Mahajan, *Scr. Mater.* **75**, 1 (2014).
- ⁷⁸F. C. Massabuau, S. L. Rhode, M. K. Horton, T. J. O'Hanlon, A. Kovács, M. S. Zielinski, M. J. Kappers, R. E. Dunin-Borkowski, C. J. Humphreys, and R. A. Oliver, *Nano Lett.* **17**, 4846 (2017).
- ⁷⁹S. Chichibu, T. Onuma, T. Sota, S. DenBaars, S. Nakamura, T. Kitamura, Y. Ishida, and H. Okumura, *J. Appl. Phys.* **93**, 2051 (2003).
- ⁸⁰R. Vetary, N. Q. Zhang, S. Keller, and U. K. Mishra, *IEEE Trans. Electron Dev.* **48**, 560 (2001).
- ⁸¹I. L. Krestnikov, N. N. Ledentsov, A. Hoffmann, D. Bimberg, A. V. Sakharov, W. V. Lundin, A. F. Tsatsul'nikov, A. S. Usikov, Z. I. Alferov, Y. G. Musikhin, and D. Gerthsen, *Phys. Rev. B* **66**, 155310 (2002).
- ⁸²X. Chen, B. Henderson, and K. O'Donnell, *Appl. Phys. Lett.* **60**, 2672 (1992).